

Report of Test

Absolute Spectral Radiance Responsivity

of the

L-1 DET-8 #107 InGaAs Radiometer

Request Submitted by:

Joel McCorkel

NASA Goddard Space Flight Center

Greenbelt, MD

1. Description of Calibration Items

The L-1 DET-8 (S/N 107) radiometer is an apertured InGaAs radiometer with a removable foreoptic to convert from measuring irradiance to radiance. The InGaAs detector is temperature stabilized with a provided L-1 model 3100 Temperature Controller. An L-1 transimpedance amplifier (model 3300v2 S/N 3300v2-026) was also provided and used during the calibration.

1.1 Calibration Request

The requested calibration is for absolute radiance responsivity from 950 nm to 1650 in 5 nm steps with best effort uncertainties.

2. Description of Test

The DET-8 detector was characterized for absolute spectral radiance on the NIST facility for Spectral Irradiance and Radiance responsivity Calibrations using Uniform Sources (SIRCUS).^{1,2} The calibration took place from August 23, 2017 to November 22, 2017. The DET-8 was on the calibration bench with transfer standards IGA2017a and Reyer trap T-01. For part of the test the SIRCUS exIGA radiometer was present. During the test the DET-8 was temperature controlled at -19.0 °C and checked at the beginning and end of each calibration session.

The radiance and irradiance responsivity of an instrument differ by a geometrical factor related to its design. As SIRCUS is optimized for efficient irradiance measurements we used a calibration scheme that makes the majority of measurements in irradiance mode and then uses a few radiance measurements to determine the geometric scaling factor. Radiance responsivity measurements were made at approximately 50 nm intervals and irradiance measurements were made at higher

density and scaled to the radiance measurements at tie points. Both the irradiance and radiance measurements are reported.

Description of laser systems used: The SIRCUS Ti:Saph laser was used from 700 nm to 900 nm and used the ultrasonic bath to despeckle the optical fiber. From 900 to 1700 nm the SIRCUS LBO/OPO system was used. For both lasers a BEOC laser power controller stabilized the beam to the 0.1 % level using feedback from a photodiode in the source integrating sphere, removing short term as well as long term fluctuations in the power output from the various laser sources. A Coherent WaveMaster (S/N W0385) and Bristol 521/621 wavemeters (S/N 5018 and 6208) measured the wavelength of the Ti:Saph and LBO/OPO laser sources respectively. For the OPO/LBO above 1100 nm, the signal wavelength is measured and converted to the idler.

Description of transfer standard detector: The IGA2017A transfer standard was used. It is an apertured single-element, windowless InGaAs detector. The IGA2017A was calibrated on the NIST Spectral Comparator Facility (SCF) in July of 2017.³

Description of Integrating Sphere Source (ISS): A Labsphere, 30 cm integrating sphere having a 75 mm diameter aperture was illuminated with laser light coupled through an optical fiber.

Control Program: The data was acquired using the SIRCUS Main Program v10.

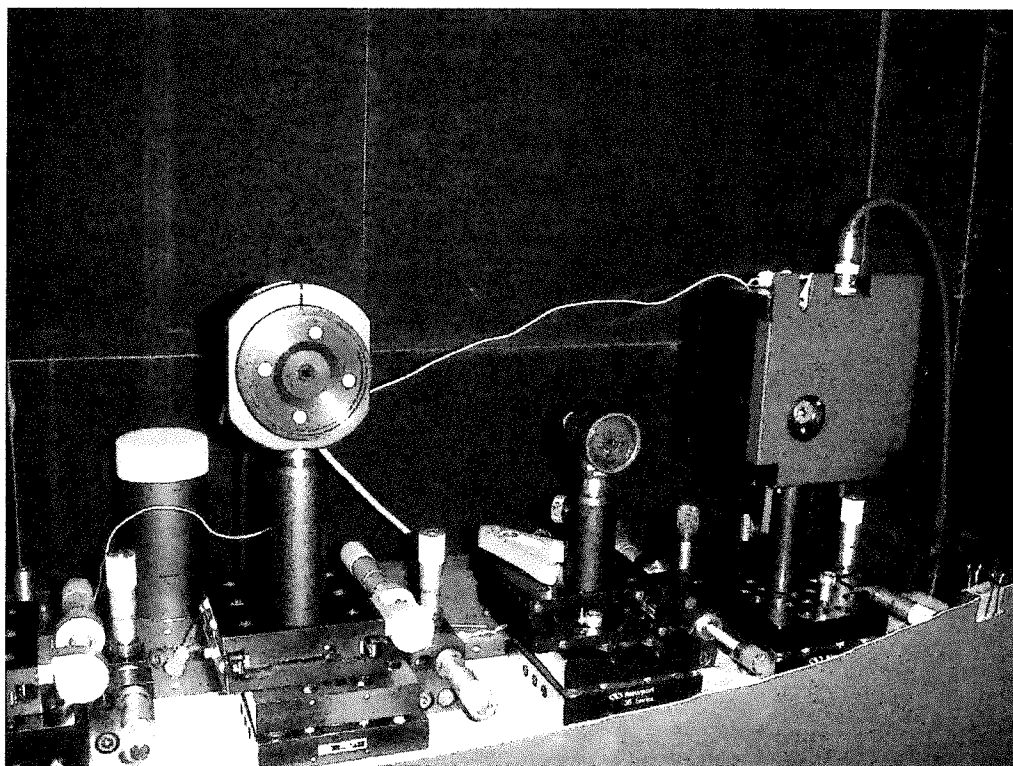


Figure 2.1. Detector bench setup. The DET-8 is on the left with its foreoptic removed.

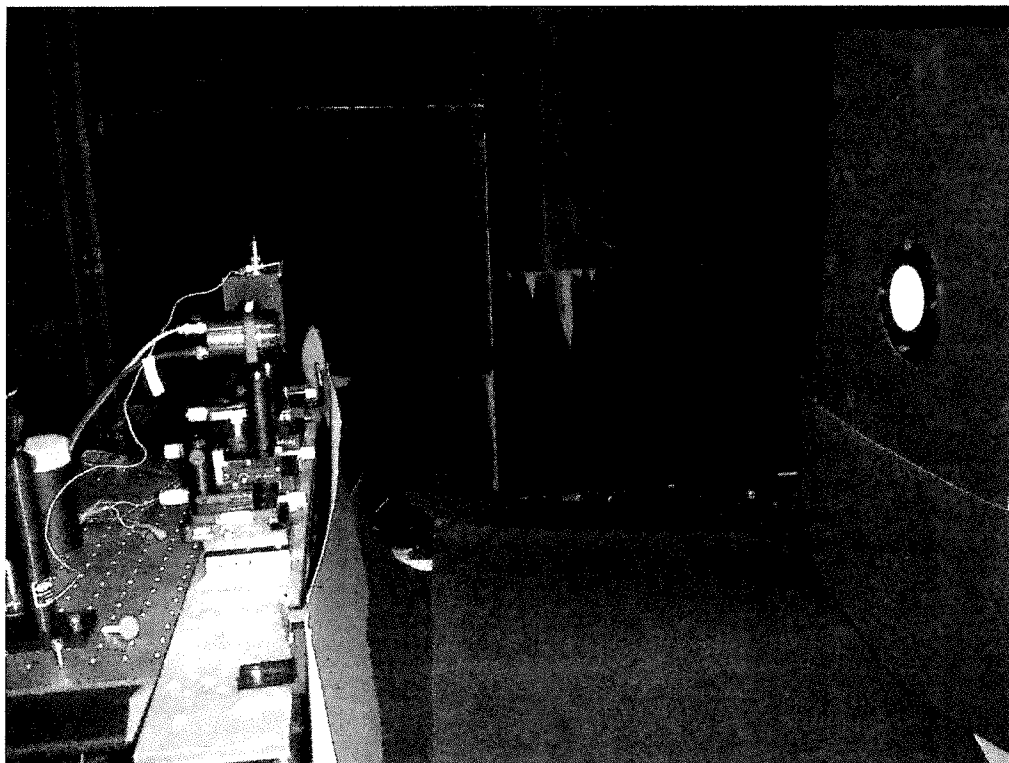


Figure 2.2. Detector bench setup (left) and integrating sphere source used in irradiance responsivity calibration (right).

2.1 Radiance Responsivity

For radiance measurements a 75 mm diameter aperture was used on the source integrating sphere and the detectors were aligned into the center of the aperture. A double headed laser was reflected off a microscope slide placed across the front of the detectors for angular alignment. The detector reference planes were determined radiometrically – see Section 3.1. Radiance measurements were taken with the source approximately 40 cm in front of the DET-8 reference plane. The source was then moved farther back to take irradiance measurements with the IGA2017A transfer standard.

2.2 Irradiance Responsivity

For irradiance measurements the same integrating sphere aperture was used. Figure 2.1 shows the DET-8, with the foreoptic removed for irradiance measurement, on the detector bench. Figure 2.2 is a cross-wise picture of the experimental setup showing the detector bench as well as the ISS used for the calibration on the right side of the figure. Measurements were made with the ISS at stage position -98.38 mm, approximately 71 cm from the detectors.

3. Results of Test

The trap detector is an irradiance meter. To measure radiance the solid angle of the source is required. To determine the solid angle, the distance between the trap aperture and the integrating sphere source aperture must be known along with the integrating sphere aperture area.

The integrating sphere is mounted on an XYZ translation stage, with the Z position measured with a linear encoder. The X and Y axes enable the source to be properly positioned in front of an instrument before it measures the sphere radiance. The Z position is used to determine the separation between relevant apertures.

3.1 Trap detector offset and offset uncertainty determination

For radiance responsivity measurements, the trap detector distance was measured radiometrically. At seven different Z positions, the trap and monitor voltages were recorded to yield a relative irradiance. From the Z position encoder reading, the actual trap aperture to sphere aperture distance in millimeters was determined using the $1/Z^2$ law for on-axis irradiance (inverse square law). The resultant data were fitted by expressions based on a point-source geometry and a non-point-source geometry (the experimental configuration). Fig 3.1 is a schematic of the configuration. Fig. 3.2 shows the point source calibration; the inverse square law fitting equation was:

$$y = \frac{m_1}{(M_0 - m_2)^2} \quad (1)$$

Where y is the relative irradiance, m_1 is a fitting constant, M_0 is Z position of the integrating sphere that is read by the Z-encoder, and m_2 is the Z position of zero offset between the two apertures. The uncertainty in m_2 , for the sphere position during calibration, gives the uncertainty in the distance between the two apertures.

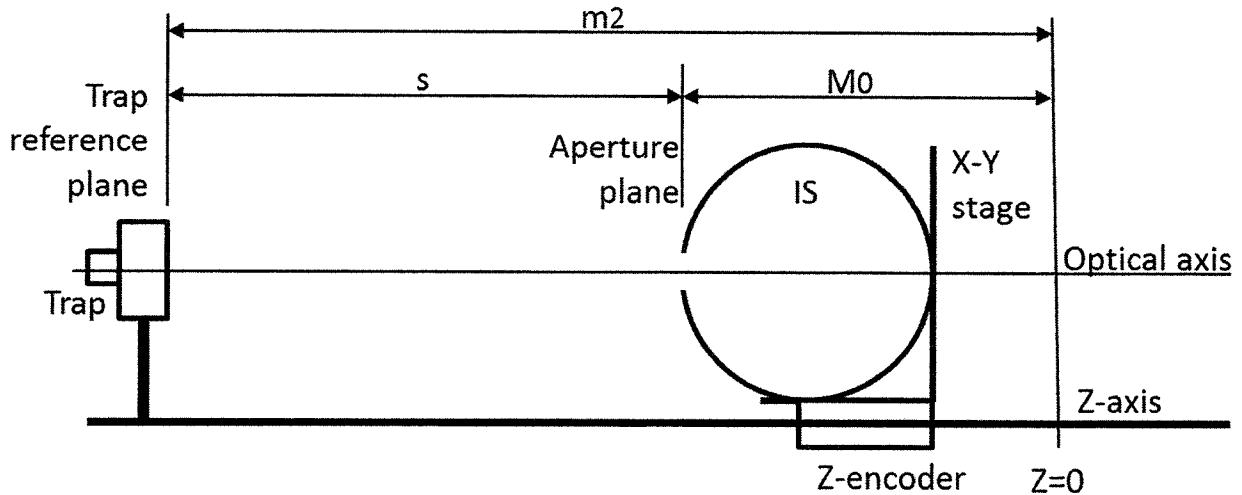


Figure 3.1. Schematic of the configuration for determining trap-sphere distance radiometrically.

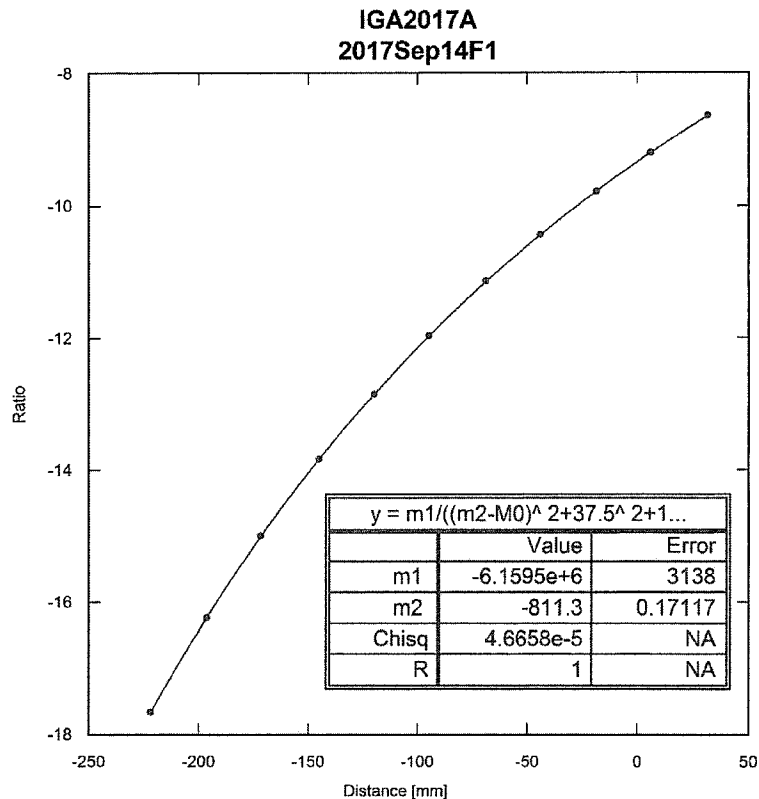


Figure 3.2. Fit of Eq. 2 to the data. Reference trap detector offset and uncertainty are shown in the inset table.

Because the source aperture was fairly large (75 mm diameter), the point source approximation was tested by fitting the following expression to the data:

$$y = \frac{m_1}{((M_0 - m_2)^2 + m_3^2 + m_4^2)} \quad (2)$$

where y , m_1 , M_0 , and m_2 are the same as in Eq. 1. $m_3 = r_d$, the radius of the trap aperture, 1.7 mm, and $m_4 = r_d$, the radius of the integrating sphere aperture, 3 mm. Equation 2 is valid in the limit where

$$(r_s^2 + r_d^2 + s^2) \gg 2r_s r_d \quad (3)$$

At a separation, s , of 50 cm, the minimum separation for the distance measurement, $(r_s^2 + r_d^2 + s^2)/2r_s r_d = 1972$, and the condition, Eq. 3, holds.

The fit to Eq. 2 has an offset, m_2 , of -811.30 mm and an uncertainty of 0.17 mm. Residuals to the fit are shown in Fig. 3.3. There is no apparent bias or offset to the residuals, and the magnitude of the residuals is less than 0.1% of the measurements themselves. Note that there is only a 0.06 mm difference in m_2 between the point source and the extended source calculations.

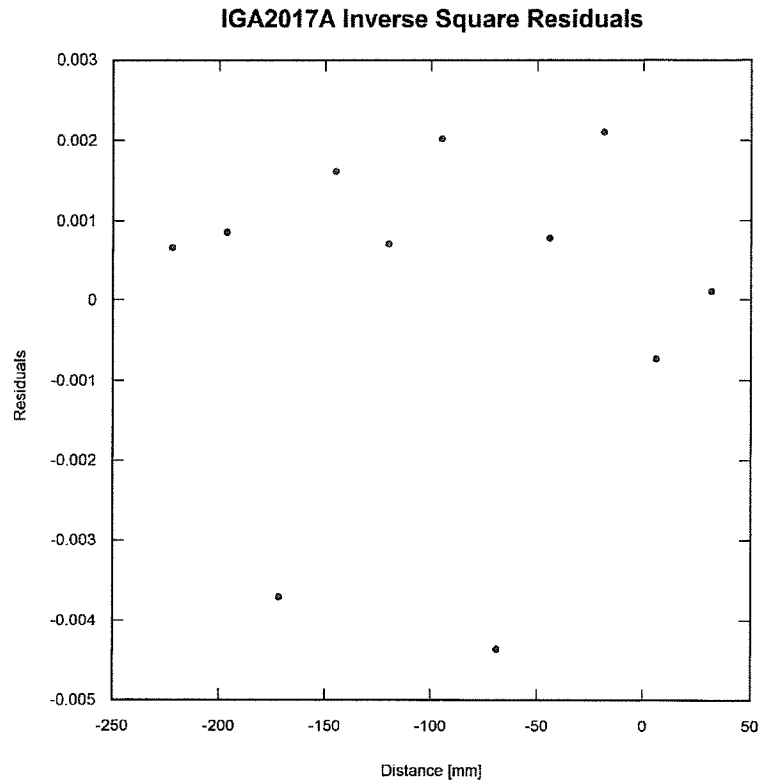


Figure 3.3. Residuals of the fit of Eq. 2 to the data.

3.2 Irradiance and Radiance Responsivity

The measured values of the irradiance responsivity of the DET-8 #107 detector are plotted in Figure 3.4 and the radiance responsivity is plotted in Figure 3.5.

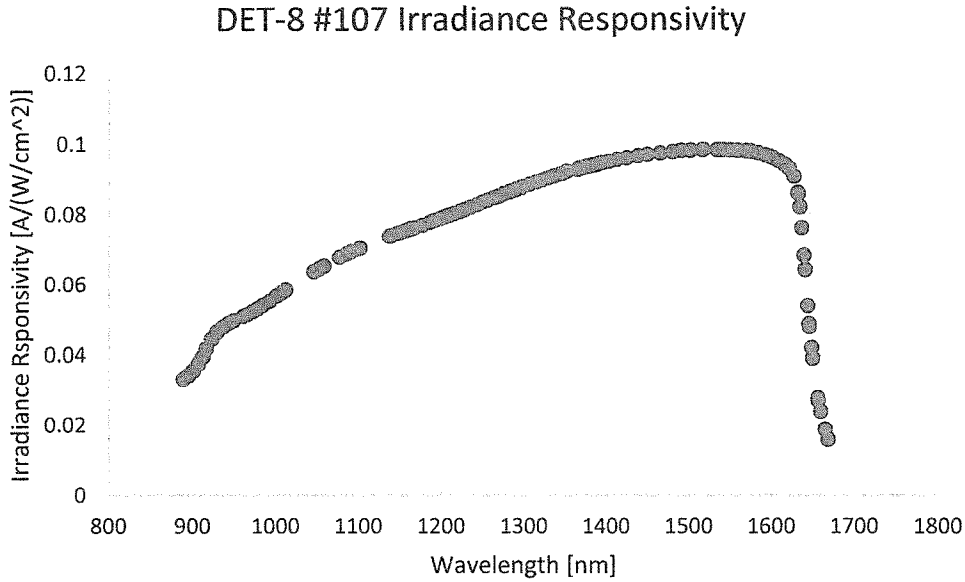


Figure 3.4 Irradiance responsivity of the DET-8 #107 radiometer.

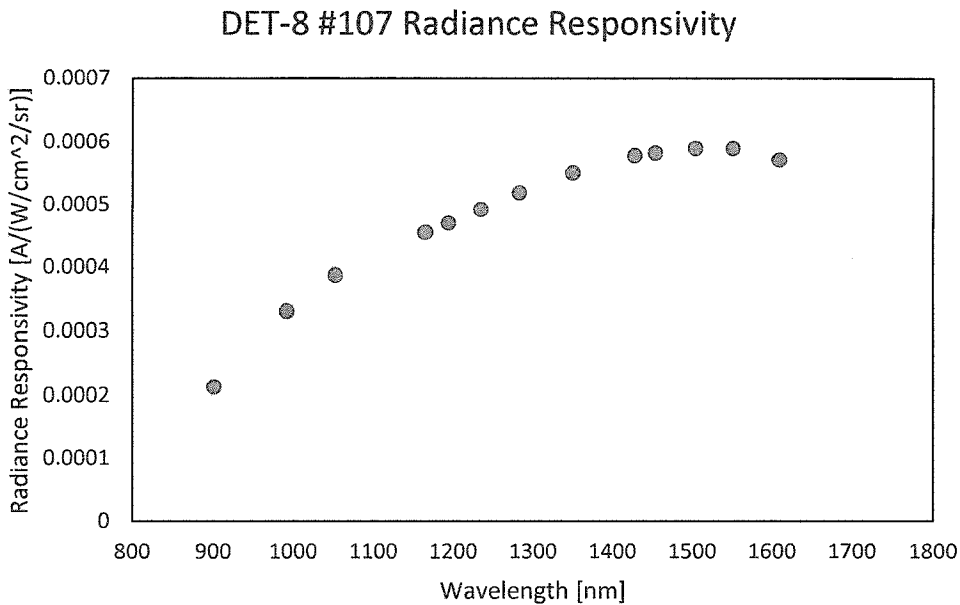


Figure 3.5 Radiance responsivity of the DET-8 #107 radiometer.

For analysis the measured values of the radiance and irradiance responsivity were entered into Kaleidagraph. The irradiance responsivity was interpolated to wavelengths at which the radiance responsivity data was collected. The ratio between the interpolated irradiance values and the measured radiance values was plotted as a function of wavelength. Ideally, this ratio is a constant. However, there is a small wavelength dependence in the ratio as seen in Figure 3.6. So, the ratio was fit to a linear function of wavelength, λ .

$$R_E = (m_1 + \lambda m_2)R_L$$

The fit values of $m_1 = 168.54(21)$ and $m_2 = -0.00128(17)$ were used to scale the irradiance responsivity measurements to radiance responsivity values.

In Figure 3.7 the radiance responsivity measurements are plotted along with the scaled values from the irradiance responsivity measurements.

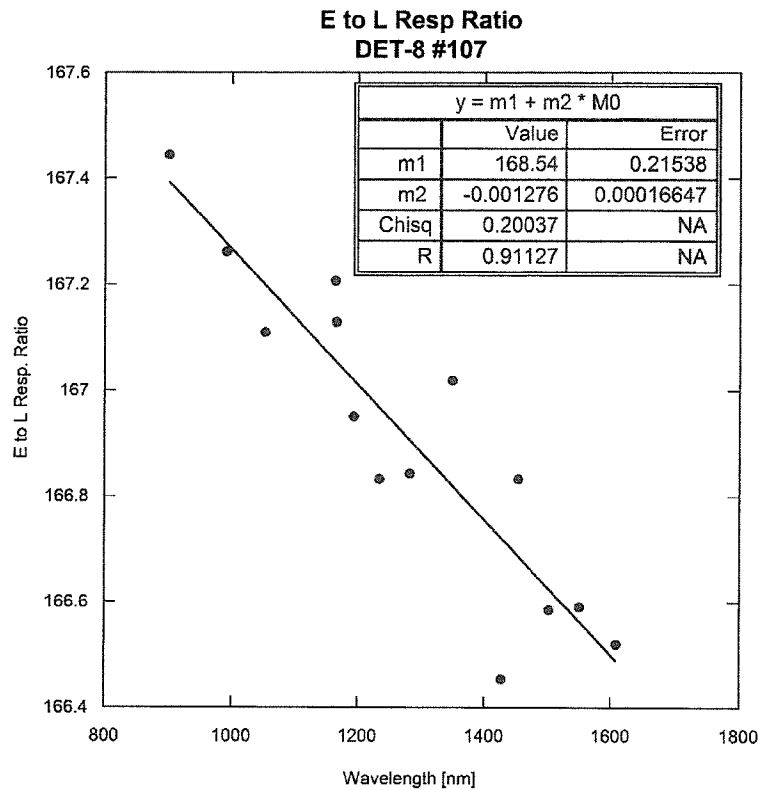


Figure 3.6 Irradiance responsivity to radiance responsivity ratio as a function of wavelength.

Radiance Responsivity of DET-8 #107

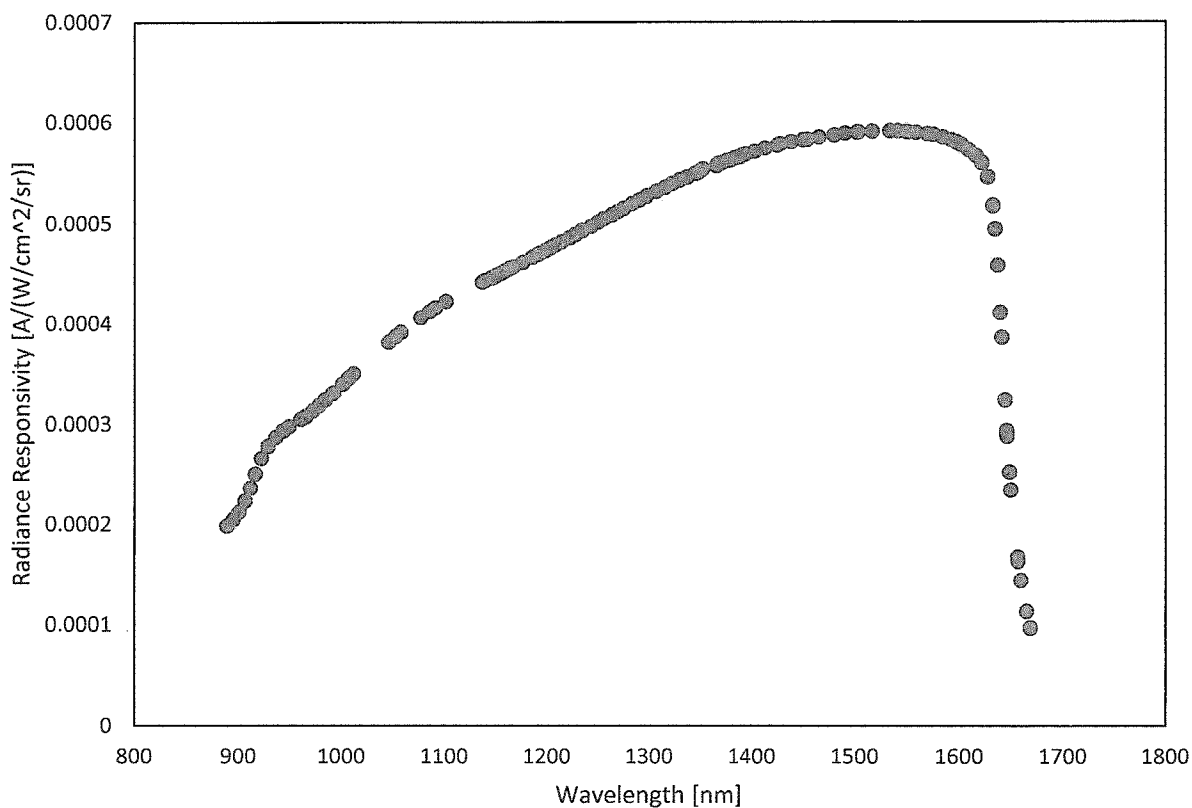


Figure 3.7. DET-8 #107 radiance responsivity. Blue circles are the measured radiance responsivity values and red circles are the scaled irradiance responsivity values.

Tabulated calibration data files were provided along with this report:

Filename: Irradiance and Radiance Responsivity DET8_107 Final.xlsx

Table 3.1 Measured radiance and irradiance responsivities and radiance responsivities interpolated to every 5 nm in wavelength.

Wavelength [nm]	Irradiance Resp [A/(cm ² /W)]	Radiance Resp [A/(cm ² /sr/W)]	Uncertainty [% k=1]	Wavelength [nm]	Radiance Resp [A/(cm ² /W)]	Uncertainty [% k=1]
888.815	3.323E-02	1.985E-04	0.79	900	2.114E-04	0.80
894.957	3.433E-02	2.051E-04	0.79	905	2.206E-04	0.80
900.408	3.556E-02	2.125E-04	0.79	910	2.317E-04	0.80
900.950	3.569E-02	2.132E-04	0.72	915	2.465E-04	0.80
906.666	3.747E-02	2.238E-04	0.79	920	2.605E-04	0.80
912.036	3.963E-02	2.368E-04	0.83	925	2.713E-04	0.80
916.441	4.193E-02	2.506E-04	0.79	930	2.795E-04	0.80
922.354	4.455E-02	2.662E-04	0.79	935	2.856E-04	0.80
928.931	4.656E-02	2.782E-04	0.79	940	2.909E-04	0.80
936.261	4.805E-02	2.871E-04	0.79	945	2.952E-04	0.80
943.506	4.912E-02	2.936E-04	0.79	950	2.986E-04	0.80
949.066	4.984E-02	2.979E-04	0.79	955	3.016E-04	0.80
960.694	5.105E-02	3.051E-04	0.79	960	3.046E-04	0.80
965.419	5.154E-02	3.081E-04	0.73	965	3.077E-04	0.73
972.366	5.246E-02	3.136E-04	0.73	970	3.120E-04	0.73
978.029	5.327E-02	3.184E-04	0.73	975	3.159E-04	0.73
984.327	5.421E-02	3.240E-04	0.73	980	3.199E-04	0.73
991.694	5.529E-02	3.305E-04	0.65	985	3.246E-04	0.73
992.594	5.542E-02	3.313E-04	0.73	990	3.294E-04	0.73
1001.175	5.686E-02	3.399E-04	0.73	995	3.335E-04	0.73
1007.019	5.782E-02	3.457E-04	0.73	1000	3.388E-04	0.73
1011.828	5.857E-02	3.502E-04	0.73	1005	3.440E-04	0.73
1045.956	6.379E-02	3.815E-04	0.72	1010	3.485E-04	0.73
1052.458	6.470E-02	3.870E-04	0.72	1015	3.528E-04	0.73
1052.486	6.473E-02	3.872E-04	0.63	1020	3.573E-04	0.73
1057.868	6.544E-02	3.914E-04	0.72	1025	3.622E-04	0.73
1076.961	6.786E-02	4.060E-04	0.72	1030	3.671E-04	0.73
1085.510	6.886E-02	4.119E-04	0.72	1035	3.720E-04	0.73
1091.122	6.949E-02	4.158E-04	0.72	1040	3.768E-04	0.73
1101.531	7.055E-02	4.221E-04	0.72	1045	3.812E-04	0.73
1136.878	7.387E-02	4.421E-04	0.73	1050	3.852E-04	0.73
1139.290	7.403E-02	4.431E-04	0.73	1055	3.888E-04	0.73
1145.816	7.451E-02	4.460E-04	0.73	1060	3.926E-04	0.73
1148.302	7.471E-02	4.472E-04	0.73	1065	3.966E-04	0.73
1150.349	7.494E-02	4.486E-04	0.73	1070	4.006E-04	0.73
1155.168	7.527E-02	4.506E-04	0.72	1075	4.045E-04	0.73
1158.914	7.563E-02	4.527E-04	0.72	1080	4.081E-04	0.73
1162.817	7.594E-02	4.546E-04	0.73	1085	4.116E-04	0.73

REPORT OF TEST
 NASA DET-8 #107

1163.353	7.612E-02	4.556E-04	0.72	1090	4.152E-04	0.73
1163.954	7.609E-02	4.555E-04	0.63	1095	4.183E-04	0.73
1165.746	7.620E-02	4.562E-04	0.63	1100	4.211E-04	0.73
1167.014	7.631E-02	4.568E-04	0.73	1105	4.240E-04	0.73
1176.529	7.709E-02	4.615E-04	0.73	1110	4.269E-04	0.73
1185.713	7.789E-02	4.663E-04	0.73	1115	4.297E-04	0.73
1191.573	7.840E-02	4.694E-04	0.73	1120	4.326E-04	0.73
1193.504	7.860E-02	4.706E-04	0.63	1125	4.355E-04	0.73
1198.470	7.901E-02	4.731E-04	0.73	1130	4.383E-04	0.73
1203.336	7.942E-02	4.756E-04	0.73	1135	4.411E-04	0.73
1204.399	7.954E-02	4.763E-04	0.73	1140	4.433E-04	0.73
1208.371	7.989E-02	4.784E-04	0.73	1145	4.456E-04	0.73
1214.095	8.039E-02	4.814E-04	0.73	1150	4.487E-04	0.73
1222.361	8.111E-02	4.857E-04	0.73	1155	4.509E-04	0.73
1228.000	8.166E-02	4.891E-04	0.73	1160	4.536E-04	0.73
1234.290	8.231E-02	4.930E-04	0.63	1165	4.555E-04	0.73
1234.863	8.230E-02	4.929E-04	0.73	1170	4.584E-04	0.73
1242.952	8.299E-02	4.971E-04	0.73	1175	4.603E-04	0.73
1249.652	8.368E-02	5.013E-04	0.73	1180	4.629E-04	0.73
1255.173	8.419E-02	5.043E-04	0.73	1185	4.656E-04	0.73
1263.355	8.488E-02	5.085E-04	0.73	1190	4.682E-04	0.73
1269.105	8.540E-02	5.116E-04	0.73	1195	4.717E-04	0.73
1275.070	8.595E-02	5.149E-04	0.73	1200	4.739E-04	0.73
1275.193	8.596E-02	5.150E-04	0.73	1205	4.763E-04	0.73
1282.766	8.665E-02	5.192E-04	0.73	1210	4.788E-04	0.73
1282.780	8.668E-02	5.194E-04	0.63	1215	4.815E-04	0.73
1290.075	8.724E-02	5.228E-04	0.74	1220	4.846E-04	0.73
1297.317	8.792E-02	5.268E-04	0.74	1225	4.874E-04	0.73
1306.808	8.872E-02	5.317E-04	0.74	1230	4.902E-04	0.73
1315.286	8.937E-02	5.356E-04	0.74	1235	4.931E-04	0.73
1322.054	8.991E-02	5.389E-04	0.74	1240	4.954E-04	0.73
1329.078	9.049E-02	5.424E-04	0.74	1245	4.982E-04	0.73
1336.423	9.099E-02	5.454E-04	0.74	1250	5.012E-04	0.73
1344.355	9.159E-02	5.490E-04	0.74	1255	5.039E-04	0.73
1347.421	9.182E-02	5.504E-04	0.74	1260	5.063E-04	0.73
1349.530	9.196E-02	5.513E-04	0.63	1265	5.091E-04	0.73
1351.949	9.237E-02	5.538E-04	0.78	1270	5.125E-04	0.73
1365.271	9.284E-02	5.566E-04	0.76	1275	5.150E-04	0.73
1366.438	9.313E-02	5.584E-04	0.76	1280	5.178E-04	0.73
1367.614	9.309E-02	5.581E-04	0.77	1285	5.202E-04	0.73
1367.631	9.318E-02	5.587E-04	0.76	1290	5.230E-04	0.73
1371.162	9.341E-02	5.601E-04	0.74	1295	5.257E-04	0.73
1375.845	9.374E-02	5.620E-04	0.74	1300	5.284E-04	0.75

REPORT OF TEST
 NASA DET-8 #107

1378.170	9.380E-02	5.625E-04	0.76	1305	5.311E-04	0.75
1378.187	9.377E-02	5.622E-04	0.76	1310	5.335E-04	0.75
1382.963	9.412E-02	5.644E-04	0.74	1315	5.359E-04	0.75
1385.369	9.422E-02	5.650E-04	0.75	1320	5.381E-04	0.75
1388.515	9.436E-02	5.658E-04	0.75	1325	5.403E-04	0.75
1391.392	9.464E-02	5.675E-04	0.74	1330	5.424E-04	0.75
1393.819	9.474E-02	5.681E-04	0.74	1335	5.444E-04	0.75
1402.836	9.516E-02	5.707E-04	0.75	1340	5.468E-04	0.75
1412.728	9.569E-02	5.739E-04	0.75	1345	5.492E-04	0.75
1424.855	9.616E-02	5.768E-04	0.76	1350	5.515E-04	0.75
1427.399	9.642E-02	5.784E-04	0.63	1355	5.557E-04	0.75
1438.015	9.674E-02	5.803E-04	0.75	1360	5.554E-04	0.75
1449.658	9.708E-02	5.824E-04	0.75	1365	5.568E-04	0.75
1453.664	9.710E-02	5.826E-04	0.63	1370	5.597E-04	0.75
1465.081	9.750E-02	5.850E-04	0.76	1375	5.617E-04	0.75
1480.062	9.783E-02	5.870E-04	0.75	1380	5.628E-04	0.75
1490.604	9.814E-02	5.890E-04	0.75	1385	5.648E-04	0.75
1501.881	9.830E-02	5.900E-04	0.75	1390	5.665E-04	0.75
1503.267	9.833E-02	5.902E-04	0.63	1395	5.684E-04	0.75
1516.523	9.842E-02	5.908E-04	0.76	1400	5.701E-04	0.75
1533.700	9.847E-02	5.912E-04	0.76	1405	5.717E-04	0.75
1541.108	9.848E-02	5.912E-04	0.76	1410	5.732E-04	0.75
1549.508	9.834E-02	5.904E-04	0.76	1415	5.746E-04	0.75
1550.539	9.830E-02	5.902E-04	0.63	1420	5.758E-04	0.75
1558.728	9.822E-02	5.898E-04	0.76	1425	5.771E-04	0.75
1569.539	9.797E-02	5.883E-04	0.76	1430	5.785E-04	0.75
1575.648	9.787E-02	5.877E-04	0.76	1435	5.795E-04	0.75
1584.238	9.744E-02	5.852E-04	0.76	1440	5.804E-04	0.75
1592.600	9.695E-02	5.823E-04	0.77	1445	5.812E-04	0.75
1597.346	9.657E-02	5.800E-04	0.77	1450	5.821E-04	0.75
1601.663	9.618E-02	5.777E-04	0.77	1455	5.833E-04	0.75
1608.683	9.529E-02	5.724E-04	0.77	1460	5.842E-04	0.75
1609.014	9.522E-02	5.720E-04	0.63	1465	5.850E-04	0.75
1615.788	9.434E-02	5.667E-04	0.77	1470	5.857E-04	0.75
1621.574	9.312E-02	5.594E-04	0.77	1475	5.863E-04	0.75
1627.223	9.079E-02	5.454E-04	0.77	1480	5.870E-04	0.75
1631.892	8.616E-02	5.176E-04	0.78	1485	5.879E-04	0.75
1632.001	8.600E-02	5.167E-04	0.77	1490	5.889E-04	0.75
1634.172	8.223E-02	4.940E-04	0.80	1495	5.896E-04	0.75
1634.178	8.220E-02	4.938E-04	0.78	1500	5.899E-04	0.75
1636.583	7.624E-02	4.580E-04	0.78	1505	5.901E-04	0.77
1639.153	6.836E-02	4.107E-04	0.78	1510	5.905E-04	0.77
1640.599	6.421E-02	3.858E-04	0.93	1515	5.909E-04	0.77

1643.769	5.392E-02	3.240E-04	0.79	1520	5.910E-04	0.77
1645.375	4.889E-02	2.937E-04	0.83	1525	5.910E-04	0.77
1645.611	4.807E-02	2.888E-04	0.80	1530	5.910E-04	0.77
1645.670	4.794E-02	2.881E-04	0.80	1535	5.910E-04	0.77
1645.767	4.826E-02	2.899E-04	0.84	1540	5.910E-04	0.77
1648.203	4.200E-02	2.524E-04	0.84	1545	5.905E-04	0.77
1649.447	3.903E-02	2.345E-04	0.79	1550	5.900E-04	0.77
1656.097	2.786E-02	1.674E-04	0.80	1555	5.900E-04	0.77
1656.642	2.707E-02	1.627E-04	0.89	1560	5.899E-04	0.77
1659.434	2.390E-02	1.436E-04	0.78	1565	5.888E-04	0.77
1664.805	1.881E-02	1.131E-04	0.89	1570	5.880E-04	0.77
1668.483	1.608E-02	9.662E-05	0.90	1575	5.881E-04	0.77
1668.555	1.606E-02	9.651E-05	0.94	1580	5.865E-04	0.77
				1585	5.847E-04	0.77
				1590	5.830E-04	0.77
				1595	5.810E-04	0.77
				1600	5.788E-04	0.77
				1605	5.752E-04	0.77
				1610	5.718E-04	0.77
				1615	5.678E-04	0.77
				1620	5.617E-04	0.77
				1625	5.518E-04	0.80
				1630	5.314E-04	0.80
				1635	4.838E-04	0.80
				1640	3.964E-04	0.80
				1645	3.011E-04	0.80
				1650	2.267E-04	0.80

3.3 Radiance Responsivity Uncertainty Analysis

To assess the uncertainties in the radiance responsivity we start with the uncertainties in the directly measured radiance responsivities. These are then summed in quadrature with the measurement uncertainties in the irradiance measurements and the uncertainties in the scaling factor applied to the irradiance measurements. Note that type B uncertainties that apply to all wavelengths in the irradiance responsivity measurements (e.g. amplifier gain and distance) are not included as the uncertainty in the scaling factor includes these sources of uncertainty.

Table 3.2 Uncertainty Budget for Absolute Spectral Radiance Responsivity

Uncertainty Component	Measured Radiance Responsivity % k=1	Scaled Radiance Responsivity % k=1
Reference detector	0.36	
TS aperture area	0.10	
TS detector uniformity	0.50	
Measurement ¹ StDevMean	0.01	
Amplifier gain	0.05	
TS to ISS Distance	0.05	
ISS aperture area	0.054	
Alignment	0.02	
Combined Standard Uncertainty	0.63	0.63
Measurement ¹ StDevMean		0.01
Scaling Factor		0.36
Wavelength		0.01
Combined Standard Uncertainty	0.63	0.73

Note 1: the percent standard deviations of each measurement for both the NIST reference standard instrument and the DET-8 are given in the calibration data files provided to the customer. These values are typical near 1200 nm.

Note 2: this is not the full DET-8 calibration uncertainty budget. The uncertainty budget, Table 3.1, does not include environmental effects on both the reference detector and the DET-8. There is no component for the wavelength uncertainty. Finally, the uncertainty budget in Table 3.2 does not include measurement uncertainties associated with the DET-8 instruments themselves. No evaluations of instrument performance characteristics such as temperature dependence, response linearity or temporal stability were performed. Also, the repeatability of switching the fore-optics between radiance and irradiance mode was not evaluated. For estimates in the interpolated uncertainty, refer to Ref. 4.

4. General Information

The integrating sphere used was a LabSphere 30.0 cm (12”) diameter, Spectralon-coated sphere equipped with a 75 mm (3”) exit aperture fabricated by LabSphere (non-point source geometry) for radiance measurements.

In irradiance mode, we checked the effect of reflected light in the SIRCUS enclosure on the detectors by placing a ‘lollipop’ between the detectors and ISS and measuring the light received by the detectors. The scattered light was < 0.1% of the total signal for all detectors. This has not been accounted for in the data reduction.

The calibration data were acquired by John Woodward and Brian Alberding using the VisSIRCUS laboratory and the VisSIRCUS data acquisition program (v10).

Information was recorded in the SIRCUS Vis #19 laboratory notebook, pp.147-152 and #20 pp. 1-9.

Data were reduced and the uncertainty tables provided were produced by John Woodward.

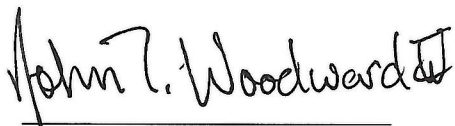
References

- [1] Brown, S. W., G. P. Eppeldauer, and K. R. Lykke, “Facility for spectral irradiance and radiance responsivity calibrations using uniform sources,” *Appl. Opt.* **45** (32) 8218-8237, (2006).
- [2] Woodward, J. T, Shaw, P.-S., Yoon, H. W., Zong, Y. Q., Brown, S. W., Lykke, K. R., “Invited article: advances in tunable laser-based radiometric calibration applications at the National Institute of Standards and Technology, USA,” *Review of Scientific Instruments* **89** 091301 (2018).
- [3] Larason, T. C., Houston, J. M., “Spectroradiometric detector measurements: ultraviolet, visible and near-infrared Detectors for spectral power,” NIST Special Publication 250-41 (2008).
- [4] Gardner, J. L., “Uncertainties in interpolated spectral data,” *J. Res. Natl. Inst. Stand. Technol.* **108**, 69-78 (2003).

This calibration report shall not be reproduced, except in full, without written approval by NIST.

Prepared by:

Approved by:



John T. Woodward, Physicist
Remote Sensing Group, 685.04
Sensor Science Division
Physical Measurement Laboratory
(301) 975-5495



Joseph P. Rice, Leader
Remote Sensing Group, 685.04
Sensor Science Division
Physical Measurement Laboratory
(301) 975-2133